2021 年臺灣國際科學展覽會
優勝作品專輯

作品編號 **160048**

參展科別 **物理與天文學**

作品名稱 **Hydrogen Functionalization of Graphene using RF Plasma for photodetection**

國　　家 **Singapore**

就讀學校 **Hwa Chong Institution**

作者姓名 **Ethan John Lim**

Qi Tianshi

Fu Wenbo

作者照片

1 Abstract

The growth of the internet is propelling an ever-increasing need for faster communication. Modern telecommunication data is mainly carried through fibre-optic cables, with pulses of light representing bits of data; the main factor limiting data transfer speed is the rate at which the optical receiver at the opposite end of the cable can detect light pulses. Graphene-silicon Schottky photodiodes are a promising alternative to traditionally-used germanium photodiodes, promising higher detection frequency and better contrast between light and dark. To make it less susceptible to erroneous measurements due to graphene having a low band gap, hydrogen functionalisation was used to increase the barrier potential of the Schottky diode so that a higher voltage would be required to allow current to pass through in forward voltage bias and trigger the sensor. This study seeks to determine the optimal conditions — of physical proximity, duration of exposure, and plasma power — for hydrogen functionalisation using radio frequency plasma. Graphene was synthesised using low pressure chemical vapour deposition, then transferred onto P-type silicon to create a photodiode. The graphene-silicon photodiode was then doped with hydrogen plasma to introduce defects in the graphene layer to increase the barrier potential of the photodiode. To assess the effectiveness of hydrogen functionalisation, photocurrent measurements were conducted while light was shone onto the photodiode in pulses of increasing frequency to find the magnitude and spontaneity of the response. Light was shone in pulses of 100ms, and was successfully detected by the photodiode. The pulse spacings were gradually decreased and it was found that the diode was able to detect pulse spacings as low as 1μs, significantly better than germanium photodetectors. The sample demonstrated clear optoelectronic response and was sensitive to changes in frequency. Results show that the intensity of the optoelectronic response in graphene-silicon diodes is inversely related to its physical proximity to the plasma source during hydrogen functionalization; and directly related to the power of the plasma and to the duration of exposure up to a point, after which it will deteriorate. Thus, it can be concluded that graphene-silicon Schottky diodes offer much promise in electronic communication.

2 Introduction

The interface between graphene and silicon has been shown to form a Schottky barrier, which exhibits rectifying properties – only allowing current to flow in one direction, enabling its use as an electrical diode (Chen *et al*, 2011). Graphene's optical transparency, along with its strong

optoelectronic response, allows the generation of photocurrent by the graphene-silicon diode when absorbing light, making it suitable for use as a high-sensitive photodetector (Wang *et al*, 2013) with higher responsiveness and improved light-to-dark current ratio (An, Behnam, & Ural, 2013). This brings great promise in the field of electronic communication, as graphene-based photodetectors have been shown to demonstrate multi-gigahertz operation over all fibre-optic telecommunication bands, exceeding existing commonly used germanium photodetectors (Pospischil *et al*, 2013). Deep sea fibre optic internet cables are carrying increasing amounts of data, requiring newer, faster networks to ensure speedy communication, thus graphene photodetectors have the potential to greatly improve fibre optics communications speeds, which currently faces low photodetection frequencies as one of the main drawbacks limiting its growth (Agrawal, 2012).

The main challenge of this application is that the barrier potential for graphene-silicon interface is lower than traditional metal-silicon junctions due to the low work function of graphene (Yan *et al*, 2012). Hydrogen plasma will be used to introduce defects onto the material surface, which will increase the barrier potential (Dey *et al*, 2016). Existing research has shown that nitrogen-doped graphene, grown through plasma-enhanced chemical vapour deposition using polydimethylsiloxane as the carbon source, can allow it to be used as the p-type layer in a diode (Wan *et al*, 2013).

3 Objectives and hypothesis

This study intends to:

- synthesise graphene using chemical vapour deposition (CVD) and create a graphene-silicon Schottky diode by transferring it onto a p-type silicon substrate; and
- investigate the optimal conditions (proximity to, power of, and duration of exposure to plasma) for hydrogen functionalisation that allows for the highest photodetection efficiency, as measured by strength and response time of photoelectric response.

This study hypothesises that:

- the graphene-silicon bilayer will display a strong photoelectric response when exposed to light, and will have higher detection frequency than traditional germanium-based photodetectors (greater than 25 GHz); and

- the photodetection efficiency of the graphene-silicon Schottky diode will be directly related to the power of the plasma and inversely related to the physical proximity and duration of exposure to the plasa source.

4 Experimental design and methodology

4.1 Synthesis of graphene-silicon diode

Few-layer graphene was synthesised using chemical vapor deposition (CVD), using methane gas as the carbon source. A 1 cm by 10 cm strip of copper was cleaned by sonication in acetone, IPA, then deionised water at 30°C for 10 minutes each. The copper strip was then placed on top of a graphene block, then into a Ø25 mm quartz tube, after which the internal pressure was reduced to 3.0 Pa (±4.0 Pa). Hydrogen gas was pumped into the tube at a rate of 2 cm^3 min^{-1}, while a heater was turned to 81.5W, 225W, then 386W at 30 minute intervals. When the temperature inside the tube reached 1100°C (± 50°C), methane gas was introduced at a rate of 10 cm^3 min^{-1}. After 1 hour, methane gas flow was stopped and the heater was turned off, allowing the tube to cool. When the temperature inside the tube reached room temperature, hydrogen gas flow was stopped and the pressure returned to ambient pressure. The graphene-coated copper strip was removed and stored in a humidity- and temperature-controlled cabinet. The CVD setup is shown in *Fig 1*.

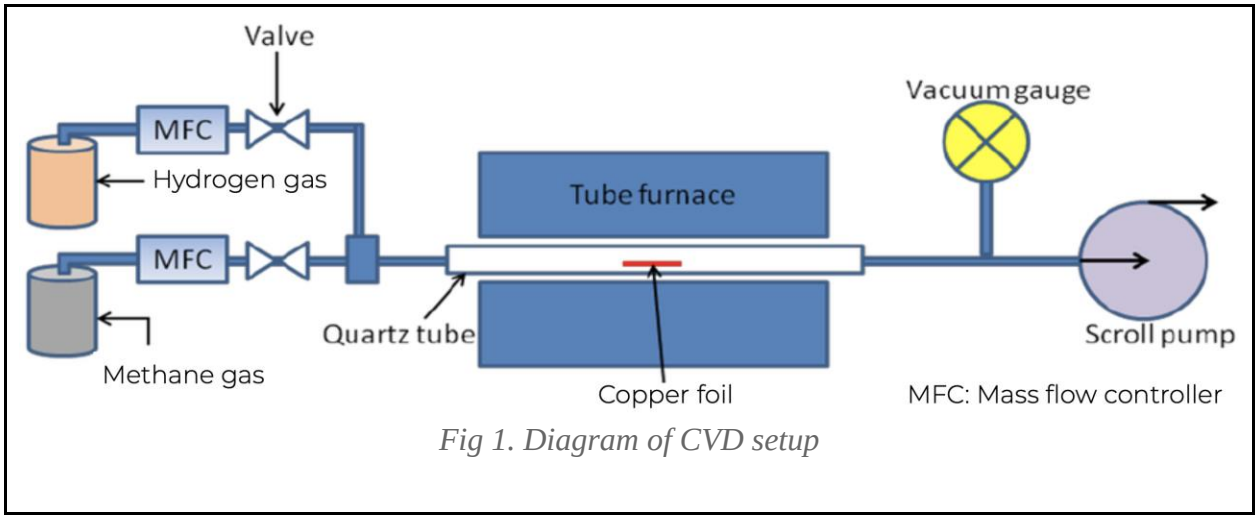

Fig 1. Diagram of CVD setup

To create a graphene-silicon diode, the graphene layer was to be removed from the copper strip, then transferred onto a p-type silicon substrate. The graphene-coated copper strip was cut into 1 cm squares, then PMMA was spin-coated onto the graphene side. The copper squares were then placed onto the surface of concentrated iron(III) chloride solution, copper side down. When the copper was fully dissolved, the graphene/PMMA squares were lifted off the surface using glass slides, and placed onto the surface of deionised water to remove excess iron(III) chloride. 1 cm by 2 cm rectangles of p-type silicon were cut, then cleaned by sonication in acetone, IPA, then deionised water at 30°C for 10 minutes each. The graphene/PMMA squares were then lifted out of the water atop the cut and cleaned silicon pieces, then placed in an incubator at 80°C for 10 minutes to remove excess moisture. The silicon pieces were then placed in acetone to allow the PMMA to dissolve, leaving a graphene-silicon bilayer. The transfer process is shown in *Fig 2*.
Raman spectroscopy and current-voltage (I-V) measurements were done on the graphene-silicon bilayer to ensure that few-layer graphene had been synthesised, and had formed a Schottky diode with the p-type silicon substrate.

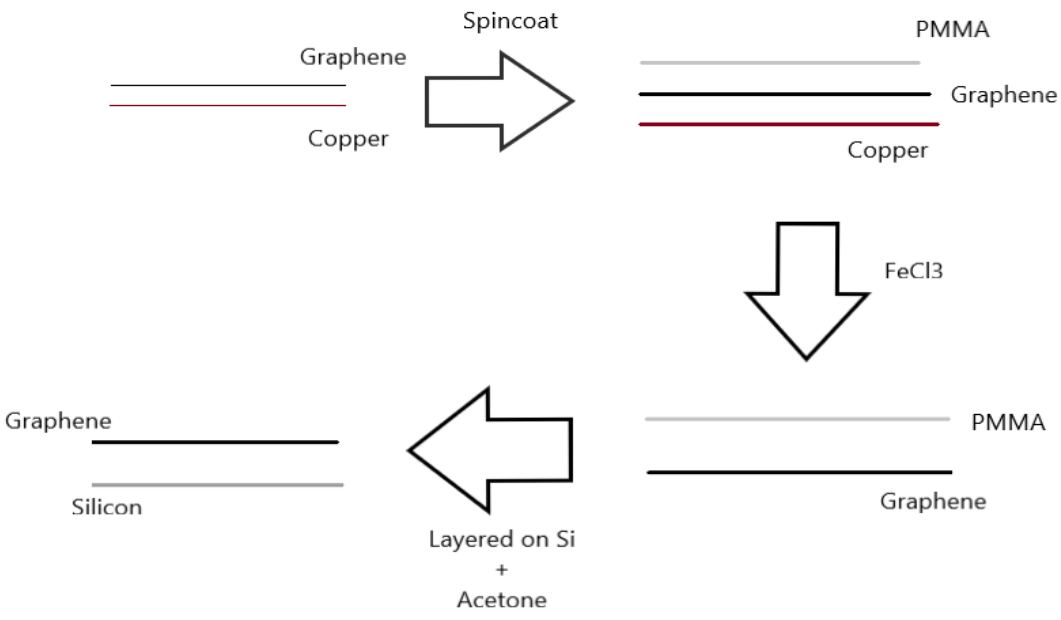

Fig 2. Diagram of Transfer process

4.2 Hydrogen functionalisation

Hydrogen functionalisation was explored as a potential method of increasing the barrier potential of the graphene-silicon diode. It involves doping the surface of graphene with hydrogen atoms using radio-frequency hydrogen plasma. The graphene-silicon diode was placed in a ceramic holder, then into a Ø25 mm quartz tube, after which the internal pressure was reduced to 100.0 Pa (±100.0 Pa). Hydrogen gas was pumped into the tube at a rate of 50 cm^3 min^{-1}, and current was then passed between two electrodes wrapped around the outside of the tube. The proximity of the diode to the electrodes, and the power and duration of the plasma were modified for each experiment. Once the required time had elapsed, the plasma and hydrogen gas flow were stopped, and pressure was returned to ambient pressure, after which the hydrogenated graphene-silicon diode was removed from the quartz tube. The hydrogenation setup is shown in *Fig 3*.

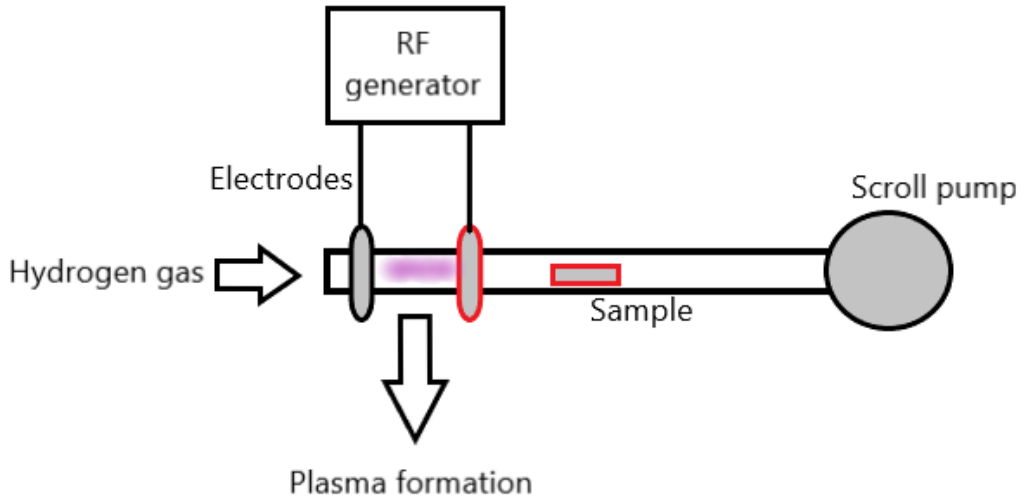

Fig 3. Diagram illustrating hydrogenation setup

The following variables were used during hydrogen functionalisation:

Independent variables	• Physical proximity from plasma electrodes • Power of plasma • Duration of exposure to plasma
Dependent variables	• Strength of photoelectric response • Response time
Controlled variables	• Growth condition of graphene samples • Silicon substrate

4.3 Current-voltage measurements

To determine the optoelectronic response, the Schottky diode, I-V measurements were taken using an I-V machine. The cathode and anode of the I-V machine were placed onto the graphene and exposed silicon of the diode respectively. The environment around the diode was then darkened to reduce interference from other light sources on the results. A voltage bias test was then done on the diode, while an LED light above the diode was turned on and off at 10 second intervals. A graph of current against time was plotted based on experimental data, using which the difference in current in light and dark could be determined *Fig 4*.

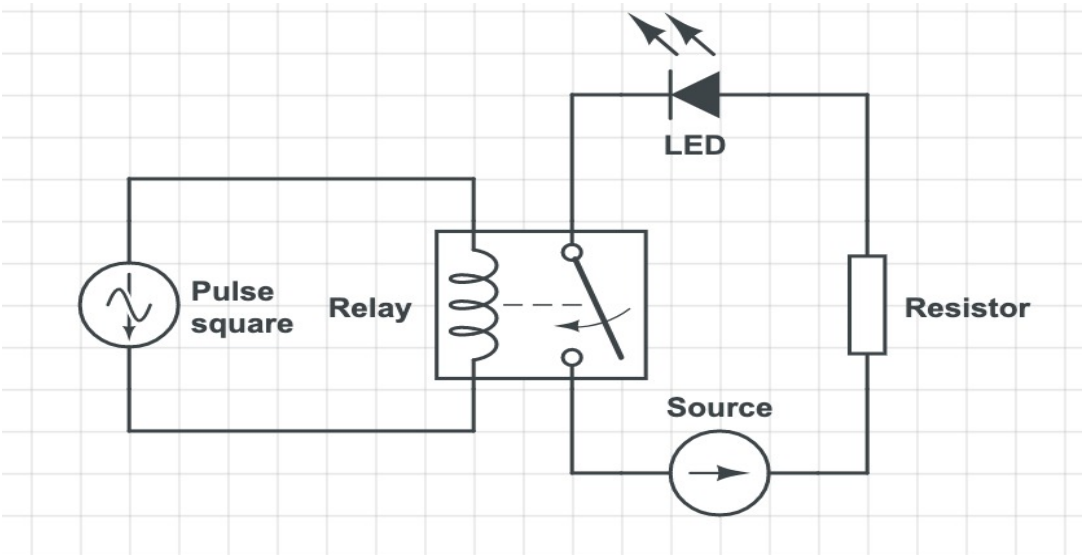

Fig 4. Schematic of detection frequency tester.

5 Results and discussion

5.1 Characterisation

5.1.1 Raman spectroscopy

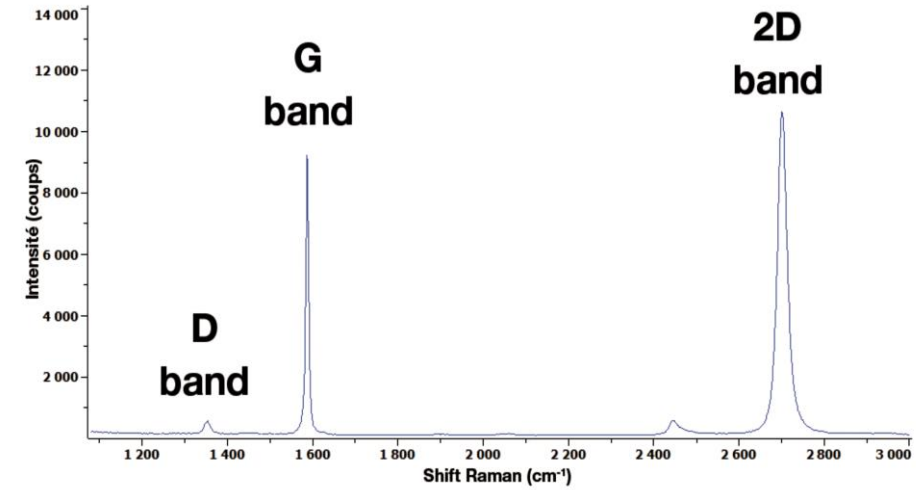

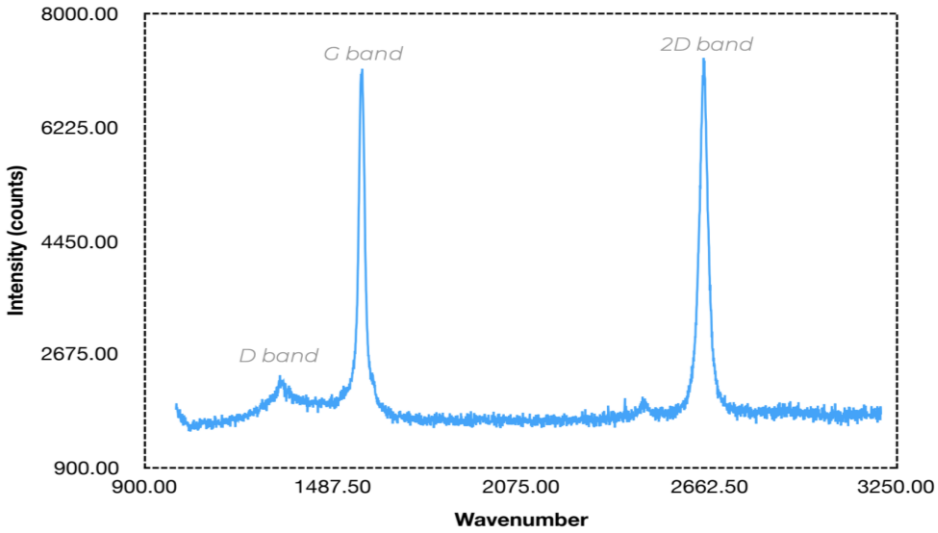

Fig 5a. (above) Raman graph for ideal graphene, obtained from literature
Fig 5b. (below) Raman graph obtained from synthesised graphene

Characterisation of graphene was done using Raman spectroscopy, where the graph obtained from the sample was compared with literature graphs for ideal graphene. Results are shown in *Fig 5a* and *Fig 5b*. *Fig 5b* clearly shows significant peaks from the D band, G band, and 2D band, as seen in the literature graph in *Fig 5a*, confirming the successful synthesis of few-layer graphene.

5.1.2 IV characterisation

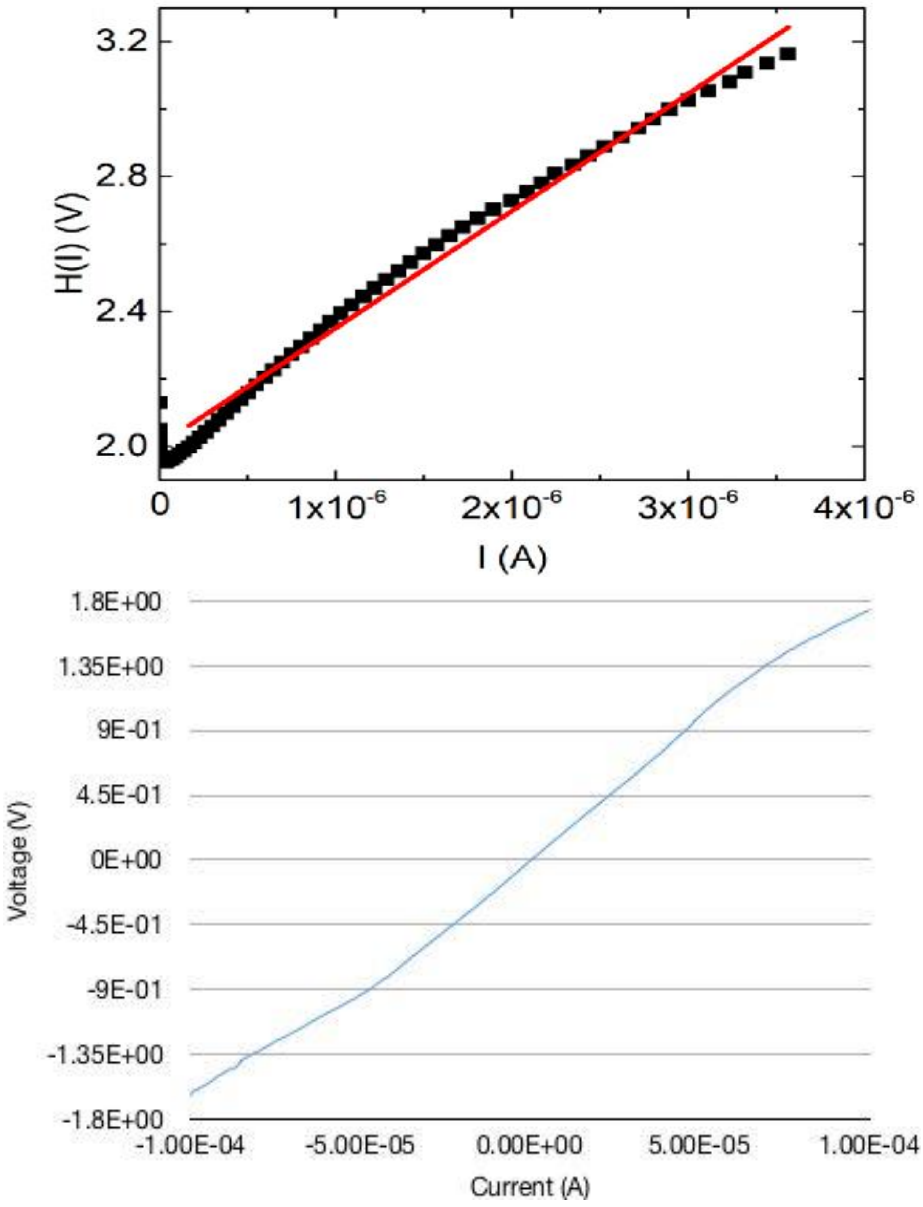

Fig 6a. (above) Literature I-V graph for ideal graphene.
Fig 6b. (below) I-V graph obtained from synthesised graphene

I-V measurements were conducted on the synthesised graphene sample using an I-V machine, and compared with existing literature. *Fig 6b* shows that the synthesised graphene has a similar I-V graph to ideal graphene, showing that the synthesised graphene has similar electrical properties to graphene, suggesting the successful synthesis of few-layer graphene.

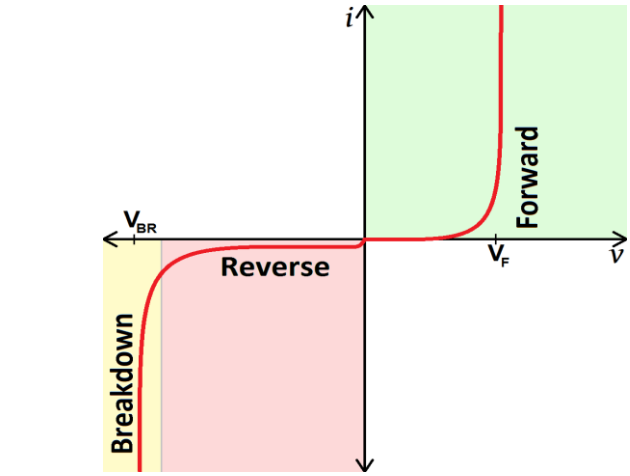

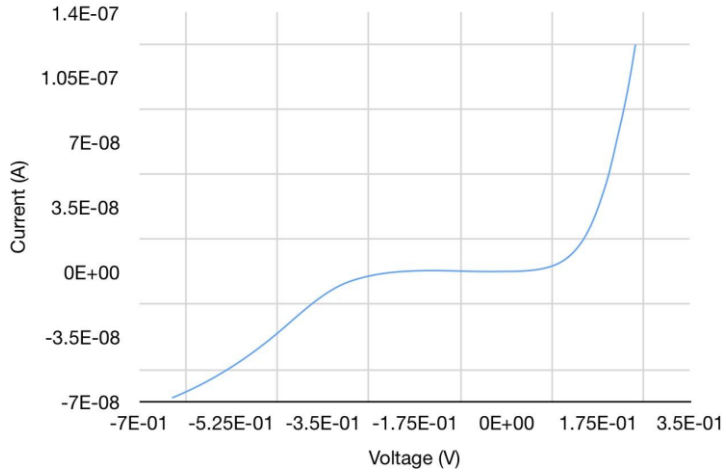

Fig 7a. (above) Literature I-V graph for ideal graphene-silicon diode
Fig 7b. (below) I-V graph obtained from synthesised graphene-silicon diode

To confirm that the graphene-silicon bilayer had successfully formed a Schottky diode, I-V measurements were conducted to determine its electrical properties, whose results are shown in *Fig 7a and Fig 7b*. The similar shapes of graphs from *Fig 7a* and *Fig 7b* show that the synthesised graphene demonstrates the expected electrical properties of an electrical diode, as seen from the sudden increase in current once the forward voltage was reached, and the backwards flow of current at the breakdown voltage. The synthesised diode has the added benefit of having a relatively low forward and breakdown voltage, hence allowing lower forward voltages to pass through and being more resistant to electrical flow in the reverse direction.

5.1.3 Ultraviolet photoelectron spectroscopy

The graphene samples on P-type silicon were examined under Ultraviolet photoelectron spectroscopy to characterise the graphene sample synthesised.

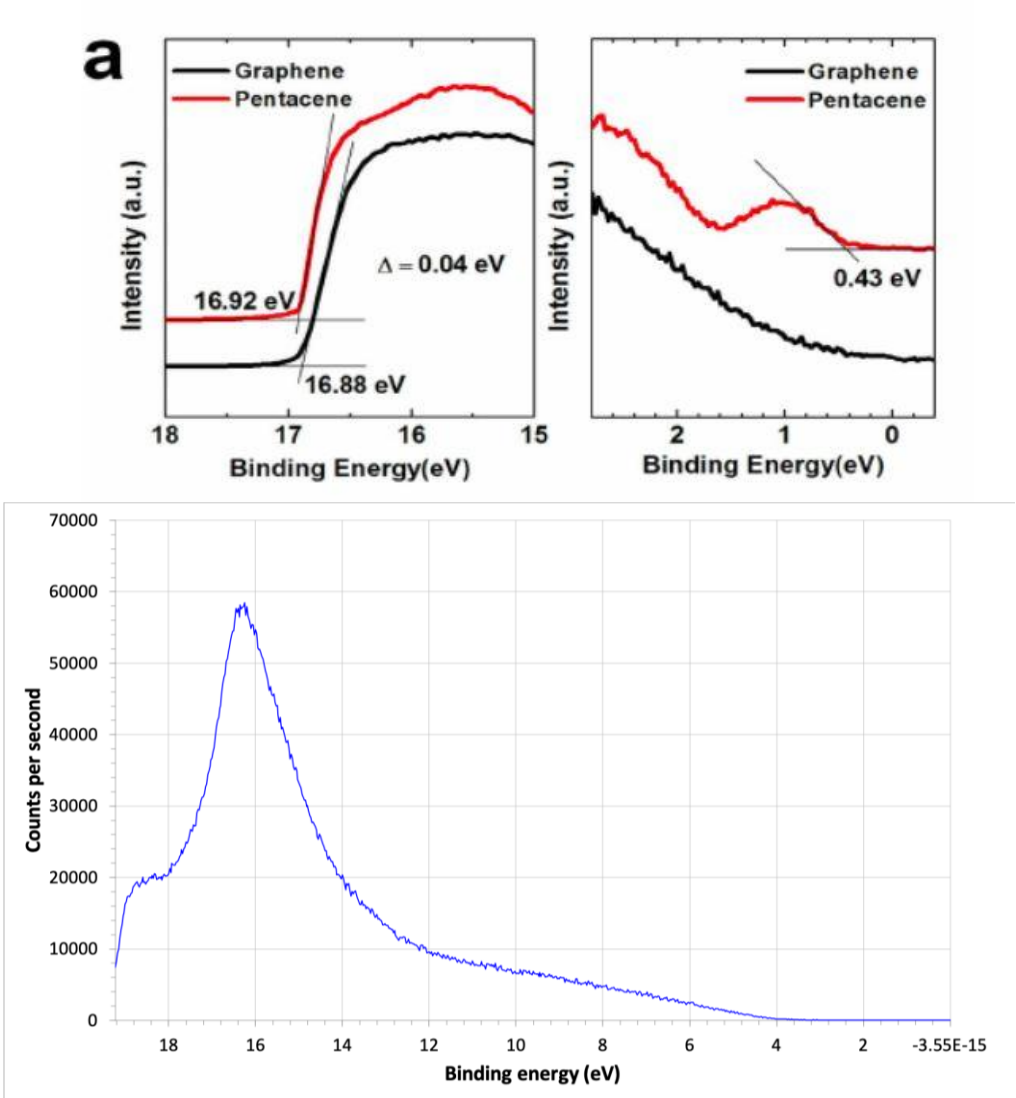

Fig 8a. (above) Literature UV photoelectron spectroscopy graph obtained from literature.
Fig 8b. (below) UV photoelectron spectroscopy graph obtained from sample.

Comparing the UV photoelectron spectroscopy graph from literature with that for the sample, it is possible to see that the sample has the same binding energy at approximately 16 eV, hence showing that graphene has been successfully synthesised.

5.2 Hydrogen functionalisation

For each experiment, to obtain the mean difference between the current measured in high and low light intensity environments, the average of all light-off data values was subtracted from the average of all light-on data values.

Proximity / cm	Duration / min	Power / W	Mean Difference / A
-	-	-	8.46×10^{-8} (control)

Physical proximity test

Proximity / cm	Duration / min	Power / W	Mean Difference / A
1.0	10	100	5.72×10^{-7}
2.5	10	100	3.24×10^{-6}
5.0	10	100	3.15×10^{-6}
7.5	10	100	5.72×10^{-7}
10.0	10	100	3.37×10^{-8}

Exposure duration test

Proximity / cm	Duration / min	Power / W	Mean Difference / A
5.0	5.0	100	2.32×10^{-7}
5.0	10	100	2.76×10^{-6}
5.0	15	100	1.23×10^{-6}
5.0	20	100	9.83×10^{-8}
5.0	25	100	9.42×10^{-8}

Plasma power test

Proximity / cm	Duration / min	Power / W	Mean Difference / A
5.0	10	50	7.46×10^{-9}
5.0	10	80	1.61×10^{-7}
5.0	10	90	3.10×10^{-7}
5.0	10	100	2.48×10^{-7}
5.0	10	110	1.73×10^{-7}
5.0	10	120	1.38×10^{-7}
5.0	10	150	7.36×10^{-10}

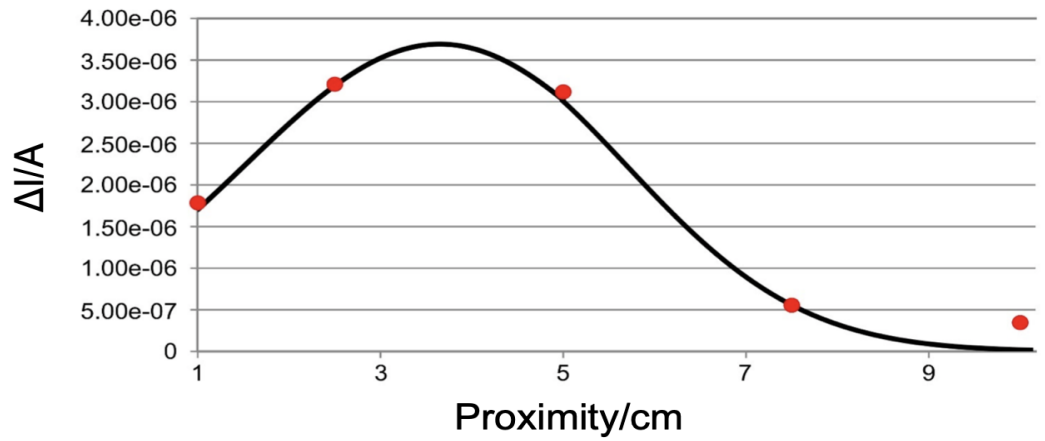

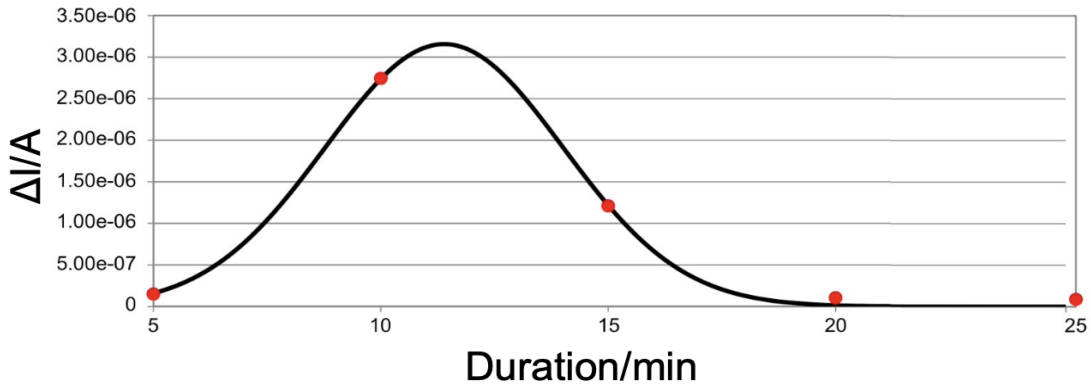

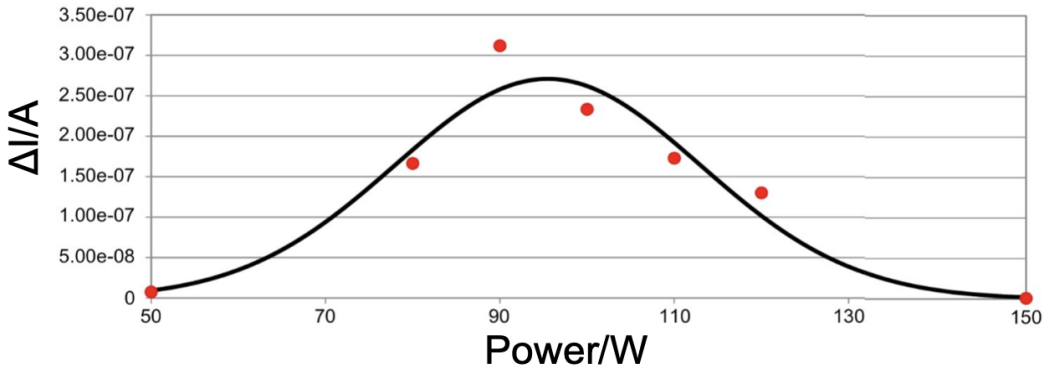

Fig 9a. (above) Effect of proximity to plasma on change in current under biased voltage
Fig 9b. (centre) Effect of duration of exposure on change in current under biased voltage
Fig 9c. (below) Effect of plasma power on change in current under biased voltage

Based on the experimental results, it is possible to conclude that the mean difference between light and dark current generated by the graphene-silicon diode is directly related to its physical proximity to the plasma source during hydrogen functionalisation, as seen from *Fig 9a*. This is likely because closer proximity to the plasma source will result in higher exposure of the diode to hydrogen plasma, therefore encouraging doping of hydrogen atoms.

It is also possible to conclude that, up to a point, the mean difference between current generation in light and dark conditions is directly related to the power of the plasma used, but after which the optoelectronic response deteriorated again (*Fig 9c*). This is likely because the higher power of plasma gives more energy for the formation of covalent bonds between carbon and hydrogen atoms, thus engineering more defects in the graphene layer, but too high-powered plasma will damage the graphene.

At close proximity, long duration and high plasma power, excessive defects result in damage to the graphene layer. Conversely, when proximity to plasma is too low, or plasma power or duration of exposure is too low, a small band gap results in samples being easily affected by noise. As such it can be concluded that the change in current measured exhibits a bell curve relationship with physical proximity, exposure duration, and plasma power.

5.3 Detection frequency

The setup used to determine the diode's peak detection frequency was similar, where the only difference was that the pulse rate of the LED light was now controlled by an electrical relay whose signal was generated by an electronic pulse generator. The pulse rate of the LED was gradually increased for each experiment while monitoring the light-to-dark ratio, and the maximum detection frequency achievable while ensuring reliable detection was determined for each sample. The pulse width and pulse spacing was varied using the pulse generator.

A change in current detected under a bias voltage of 1.0V corresponds to the frequency in which the light is turned on and off. In Fig 10, a pulse width of 100ms was applied and the pulse spacing was changed from 100ms to 10ms then back to 100ms, which was detected by the graphene-silicon photodiode and shown in the difference in number of peaks within a certain time frame.

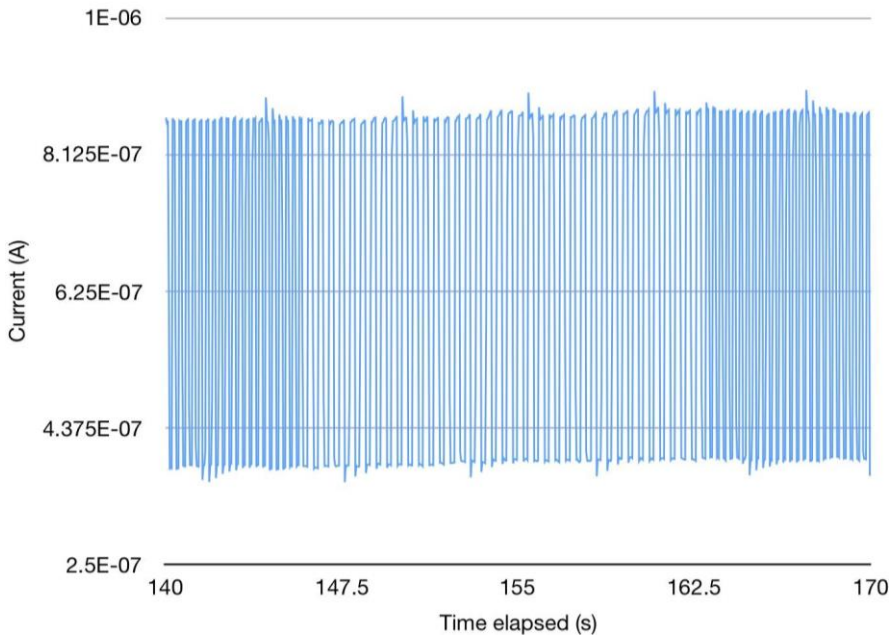

Fig 10. Frequency test with pulse width of 100ms and pulse spacing varied from 100ms to 10ms to 100ms

Results were unable to be determined for pulse widths of under 100ns due to limitations in the pulse generator used. It was found that the silicon-graphene diode was able to detect pulse spacings of as low as 1µs.

6 Conclusion

The data obtained from the experiment showed that the intensity of optoelectronic response in graphene-silicon diodes is inversely related to its physical proximity to the plasma source during hydrogenation; directly related to the power of the plasma, up to a point, after which it will deteriorate.

This study contains possible limitations, *inter alia* random experimental errors, flaws in experiment design, and lack of depth, as more data would be necessary to produce more a satisfactory and conclusive result. Further work is recommended, especially to:

- develop a process for more consistent diode fabrication;
- develop a process for more thorough removal of impurities introduced into the graphene during its transfer process;
- increase the low current generation by the photodiode when light is shone on it; and

- improve the poor lifespan of the effects of hydrogen functionalisation, as hydrogen atoms are lost to the environment within a short period of time. Dehydrogenation occurs over time due to the stressed sp3 carbon atom when it is bonded to hydrogen.

The photodetection capabilities of the graphene-silicon diode demonstrated in this study show high promise for its future development as a novel alternative to traditional photodetectors, with the potential to bring great advancements in high-volume electronic communication.

References

Agrawal, G. P. (2012). Fiber-optic communication systems (Vol. 222). John Wiley & Sons.

An, Y., Behnam, A., Pop, E., & Ural, A. (2013). Metal-semiconductor-metal photodetectors based on graphene/p-type silicon Schottky junctions. Applied physics letters, 102(1), 013110.

Chen, C. C., Aykol, M., Chang, C. C., Levi, A. F. J., & Cronin, S. B. (2011). Graphene-silicon Schottky diodes. Nano letters, 11(5), 1863-1867.

Dey, A., Chroneos, A., Braithwaite, N. S. J., Gandhiraman, R. P., & Krishnamurthy, S. (2016). Plasma engineering of graphene. Applied Physics Reviews, 3(2), 021301.

Li, X., Magnuson, C. W., Venugopal, A., Tromp, R. M., Hannon, J. B., Vogel, E. M., Ruoff, R. S et al. (2011). Large-area graphene single crystals grown by low-pressure chemical vapor deposition of methane on copper. Journal of the American Chemical Society, 133(9), 2816-2819.

Pospischil, A., Humer, M., Furchi, M. M., Bachmann, D., Guider, R., Fromherz, T., & Mueller, T. (2013). CMOS-compatible graphene photodetector covering all optical communication bands. Nature Photonics, 7(11), 892.

Wang, C., Zhou, Y., He, L., Ng, T. W., Hong, G., Wu, Q. H., ... & Zhang, W. (2013). In situ nitrogen-doped graphene grown from polydimethylsiloxane by plasma enhanced chemical vapor deposition. Nanoscale, 5(2), 600-605.

Wang, X., Cheng, Z., Xu, K., Tsang, H. K., & Xu, J. B. (2013). High-responsivity graphene/silicon-heterostructure waveguide photodetectors. Nature Photonics, 7(11), 888.

Yan, R., Zhang, Q., Li, W., Calizo, I., Shen, T., Richter, C. A., ... & Grace Xing, H. (2012). Determination of graphene work function and graphene-insulator-semiconductor band alignment by internal photoemission spectroscopy. Applied Physics Letters, 101(2), 022105.

Zhang, X., Xie, C., Jie, J., Zhang, X., Wu, Y., & Zhang, W. (2013). High-efficiency graphene/Si nanoarray Schottky junction solar cells via surface modification and graphene doping. Journal of Materials Chemistry A, 1(22), 6593-6601.

Appendix

Fig A1a - A1m: current graphs obtained from samples. Parameters of hydrogenation are written underneath in this format (proximity to plasma source, duration of exposure, power of plasma):

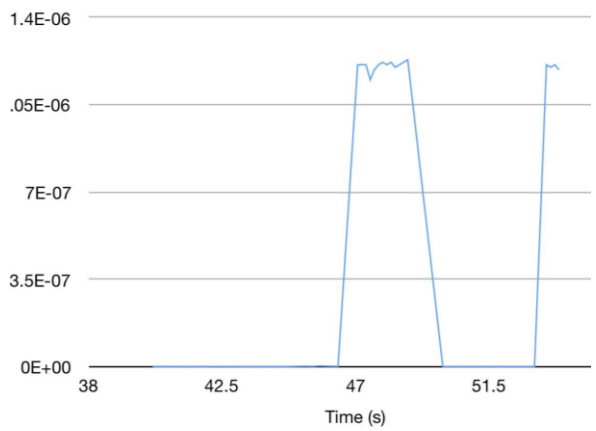

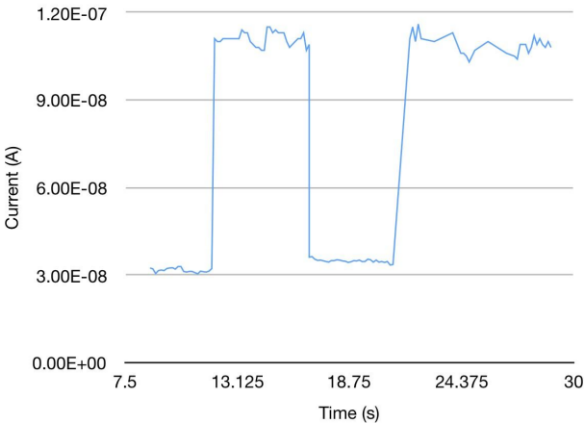

Fig A1a (left). 1 cm, 10 min, 100 W
Fig A1b (right). 5 cm 10 min, 100 W

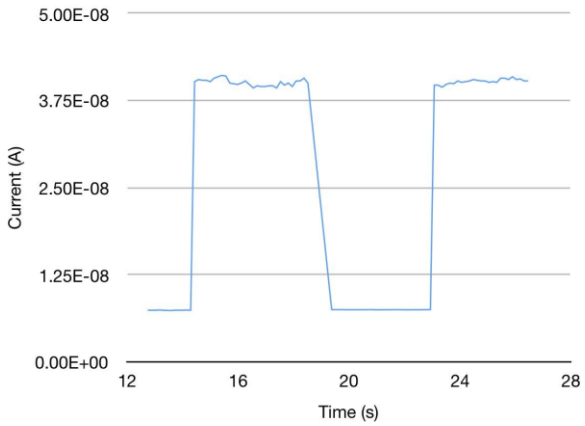

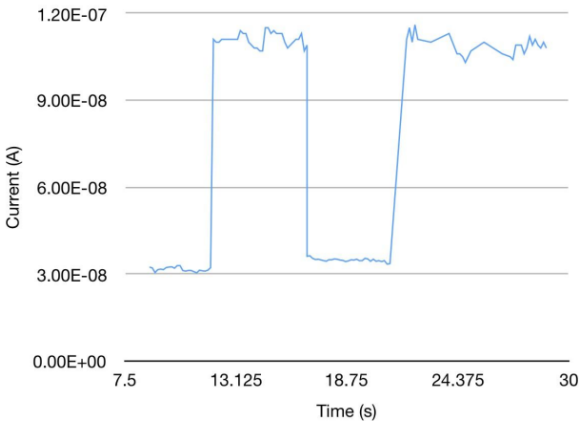

Fig A1c (left). 10 cm, 10 min, 100 W
Fig A1d (right). 5 cm, 10 min, 100 W

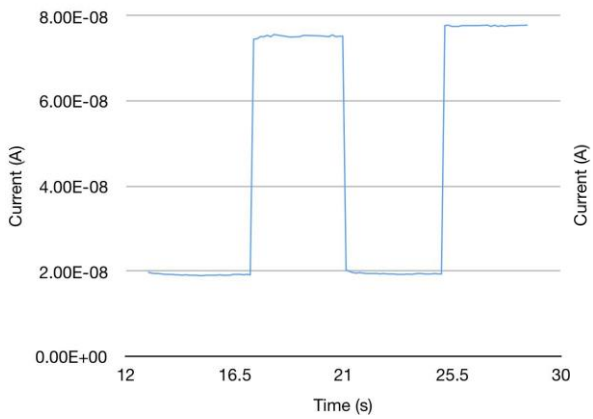

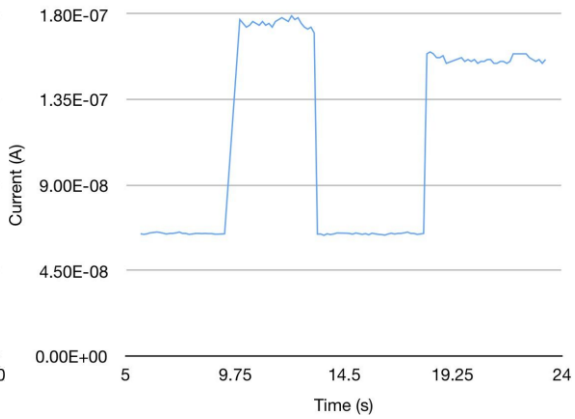

Fig A1e (left). 5 cm, 15 min, 100 W
Fig A1f (right). 5 cm, 20 min, 100 W

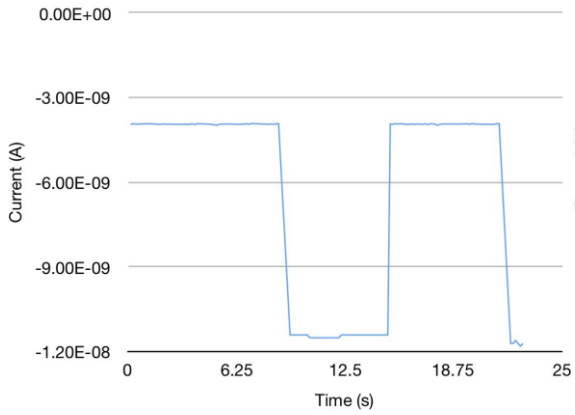

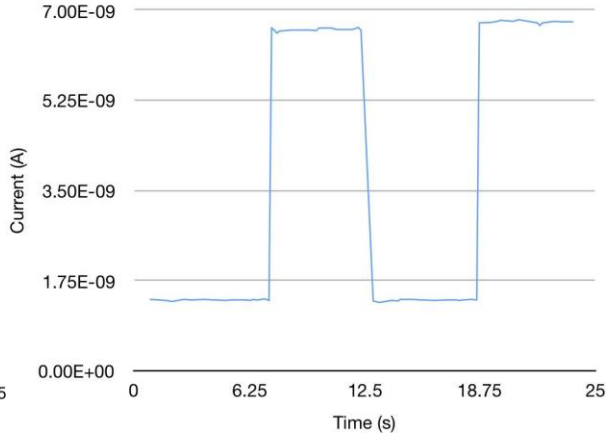

Fig A1g (left). 5 cm, 10 min, 50 W
Fig A1h (right). 5 cm, 10 min, 80 W

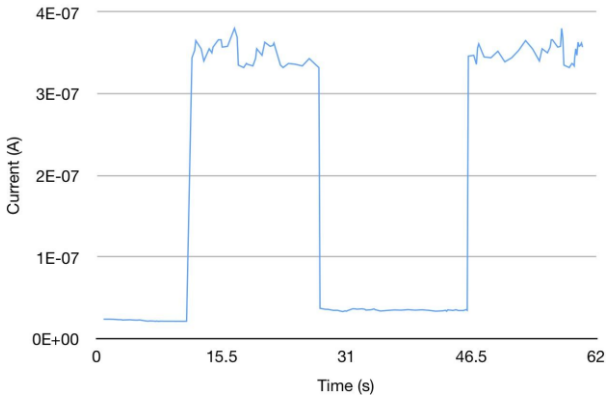

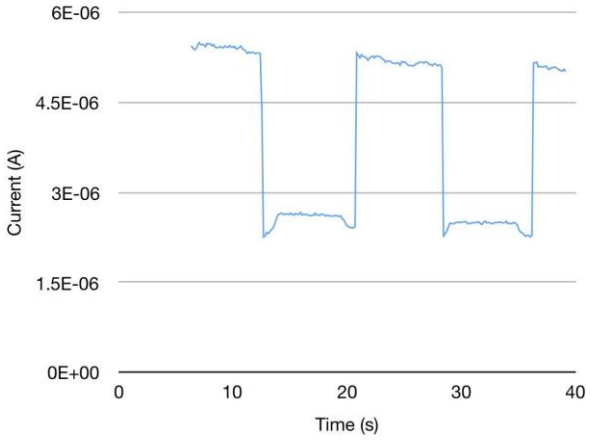

Fig A1i (left). 5 cm, 10 min, 90 W
Fig A1j (right). 5 cm, 10 min, 100 W

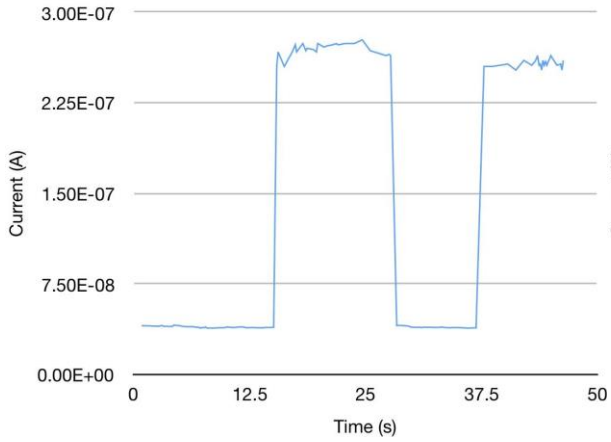

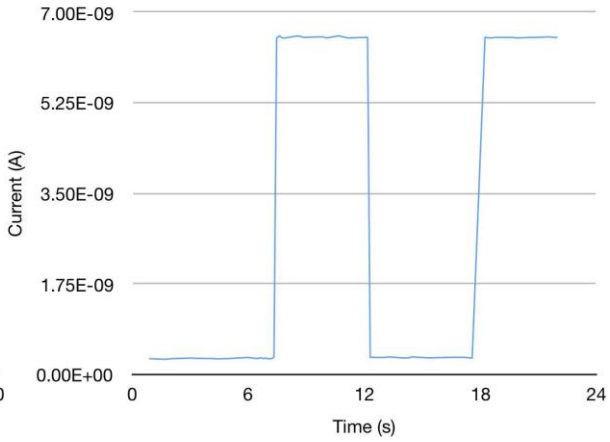

Fig A1k (left). 5 cm, 10 min, 110 W
Fig A1l (right). 5 cm, 10 min, 120 W

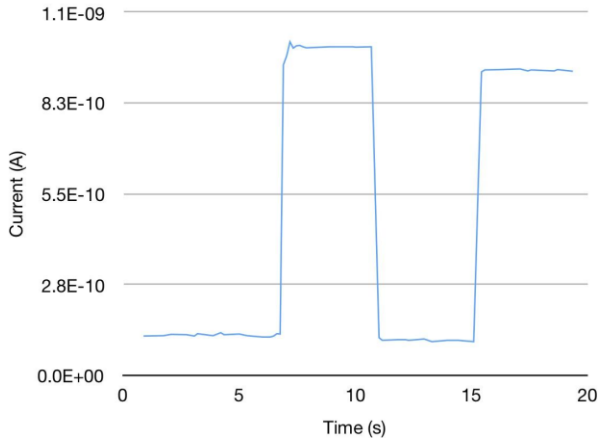

Fig A1m. 5 cm, 10 min, 150 W

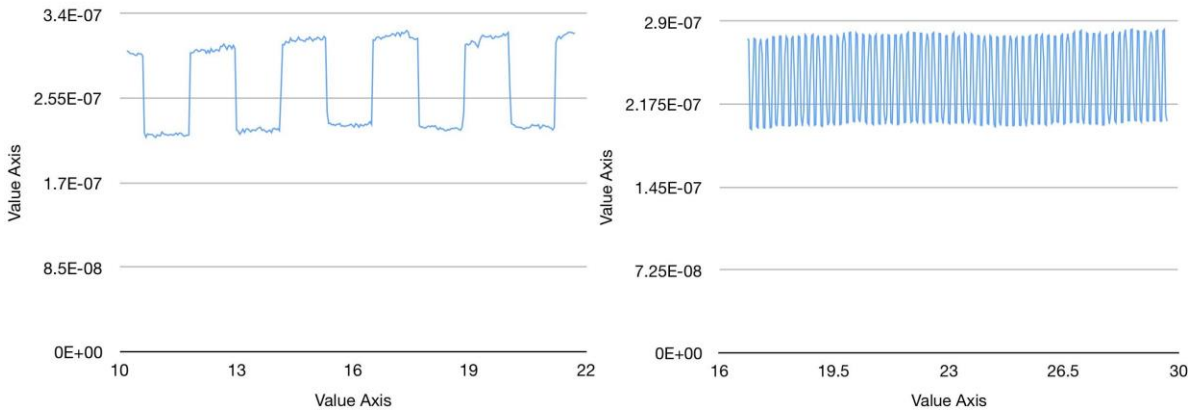

Fig A2a (left). Current graph while varying pulse width and pulse space at 100 ms and 100 ms respectively, showing consistent plateaus for both light and dark conditions

Fig A2b (right). Current graph while varying pulse width and pulse space at 100 ms and 10 µs respectively, showing level consistent ratios between light--to-dark current.

【評語】160048

The authors aim to develop graphene-based photo-detector with improved photocurrent to dark-current ratio and peak detection frequency. Unfortunately, graphene-based device exhibits inherently low barrier potential, thus hydrogenation of the CVD-grown graphene is further proposed to overcome this problem.

The authors have employed radio-frequency hydrogen plasma treatments, under different plasma power, duration, and proximity, to control and optimize the degree of hydrogenation. Direct measurements of the photocurrents as a function of the above-mentioned process parameters have been conducted and optimized conditions have been obtained. However, the characterizations of the samples are either not satisfactory or incomplete, for instance, Raman data for the graphene after hydrogenation, and the rectifying properties of the hydrogenated graphene-Si bilayers. Furthermore, the authors did not address fundamental questions such as the followings. Is the CVD grown graphene single layer or multi-layer? Will the graphene – based photo-detector exhibit layer-dependent properties?